[2] Poeschel, R. L., Ward, J. W., and Knauer, W., "Study and Optimization of 15 cm Kaufman Thruster Discharges," AIAA Paper 69-257, Williamsburg, Va., 1969.
[3] Kerslake, W. R., Byers, D. C., Staggs, J. F., "SERT II: Mission and Experiments," *Journal of Spacecraft and Rockets*, Vol. 7, No. 1, Jan. 1970, pp. 4–6.
[4] Moore, R. D., "Magnetoelectrostatically Contained Plasma Ion Thruster," AIAA Paper 69-260, Williamsburg, Va., 1969.

MARCH 1970 J. SPACECRAFT VOL. 7, NO. 3

Laboratory Testing of the Space-Charge-Sheath Electric Thruster Concept

R. X. MEYER*
The Aerospace Corporation, El Segundo, Calif.

Recent experimental results obtained with a laboratory model of the space-charge-sheath thruster are reported. The principal feature of this thruster is the electrostatic acceleration of ions in a space-charge sheath that is formed on the ionizer. The range of operating conditions tested was as follows: specific impulse = 2700–5500 sec; magnetic field strength = 800–2500 gauss; accelerating gap = 1–3 mm; ionizer surface = 13.8 cm²; cesium vapor pressure = 5–38 mm Hg; ion-beam current density = 4–14 ma/cm². The resulting ion-beam has been found to be surprisingly well collimated, with an estimated half angle of 1.5°. Under best operating conditions, the electron drain current to the anode (ionizer) was 31% of the total current.

Introduction

EXPERIMENTAL results obtained with a laboratory model designed to test the space-charge-sheath electric thruster concept are reported. The operating mode of this device and some initial experimental results have been described previously.[1,2]

Cesium ions, which are produced by contact ionization on a hot tungsten surface, are accelerated electrostatically in the space-charge sheath formed between the ionizer and the beam plasma (Fig. 1). No accelerating electrodes are employed; instead, a heated tungsten filament is used for electron emission and a transverse magnetic field serves to suppress the electron current to the ionizer. The emitting filament can be located at a relatively large distance from the beam, thereby avoiding erosion through ion sputtering. The ionizer is at a positive potential, and the emitting filament (cathode) is grounded.

The device is operated in a regime in which the electron cyclotron radius is only slightly smaller than the gap between the ionizer and the magnetic field lines intersecting the filament. The ion cyclotron radius is so large, however, that the ions leave the strong magnetic field region before the trajectories are appreciably bent.[1]

As indicated schematically in Fig. 2, the ionizer has an annular configuration. A radial magnetic field is maintained between two concentric pole pieces. The cricular emitting filament is located near the outer periphery of the ionizer annulus.

Since, except for infrequent collisions, the electrons are free to move along the magnetic field lines, the latter are also approximate lines of constant electrostatic potential and form a virtual cathode in close proximity to and parallel to the ionizer surface. Since the spacing between virtual cathode and ionizer can be quite small (of the order of 1–3 mm), a high perveance per thruster module is possible.

The device has some similarity to Hall current plasma thrusters.[3–7] However, in Hall current thrusters, the acceleration of the ions takes place in the interior of an electrically neutral plasma instead of in a space-charge sheath, and extends over a distance which is much larger than an electron cyclotron radius. By confining the acceleration to the space-charge sheath region, the present device attempts to avoid the plasma wall losses, which seem to be inherent in Hall current and other magnetohydrodynamic thrusters. The present device is space-charge limited, however, a property that it shares with contact and electron bombardment type ion engines.

Potential advantages of the space-charge-sheath electric thruster concept include the absence of an ion-optical structure and therefore avoidance of ion sputtering and the resulting deterioration of the accelerator electrode. The high degree of beam collimation that was observed in the experiments may be of importance in certain applications when impingement of the ion beam on other spacecraft components must be avoided.

Electron and Ion Trajectories

Under the combined influence of the axial electric and the radial magnetic fields, the electrons and ions experience an azimuthal drift. In Fig. 3 are shown computed electron trajectories corresponding to two different magnetic field strengths. These trajectories, which are qualitatively similar

Presented as Paper 69-282 at the AIAA 7th Electric Propulsion Conference, Williamsburg, Va., March 3–5, 1969; submitted March 17, 1969; revision received August 25, 1969. The author wishes to thank A. H. Wildvank who built much of the apparatus used in the reported experiments, and who collaborated in all phases of the test program. This research was supported by the U.S. Air Force under Contract F04701-69-C-0066.

* Director, Plasma Research Laboratory.

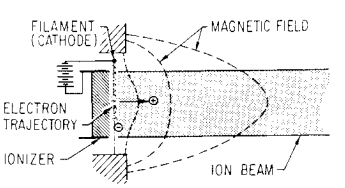

Fig. 1 Schematic diagram of space-charge-sheath electric thruster. The figure represents a radial cross section through the thruster.

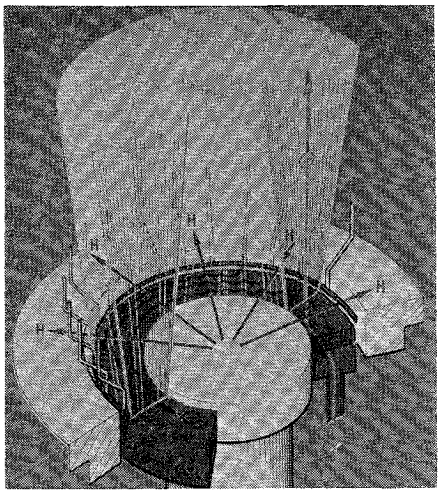

Fig. 2 Schematic diagram showing annular ionizer with cesium vapor feed, circular emitting filament (cathode), and magnetic pole pieces. (H = magnetic field in the accelerating region.)

to cycloids, were computed on the basis of a self-consistent electric field, i.e., a field in which the combined space-charge of electrons and ions is taken into account.[1]

The ion cyclotron radius is much larger than the characteristic scale length of the magnetic field; hence, the ions describe an approximately rectilinear path, perpendicular to the ionizer surface.

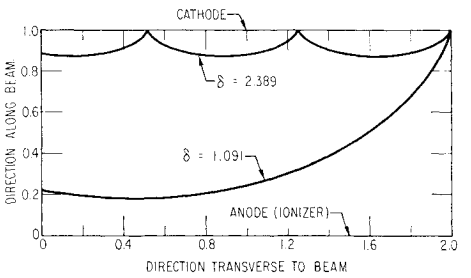

Fig. 3 Computed electron trajectories in the accelerating region of the space-charge-sheath thruster. The trajectories, which are qualitatively similar to cycloids, are the trajectories for a self-consistent field solution. (δ = magnetic field parameter.)

Experimental Apparatus

The thruster apparatus was installed in a vacuum chamber. Micrometer screws permit exact axial positioning of the ionizer, of the inner pole piece and of an electrostatic probe, during operation of the thruster.

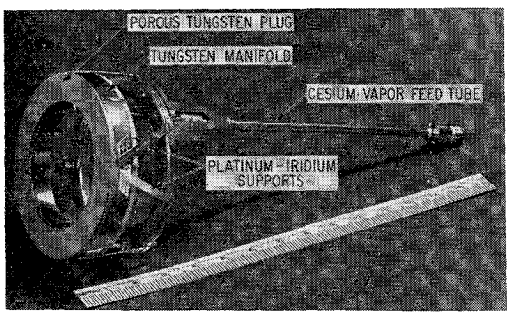

Fig. 4 Annular porous-tungsten ionizer. Nominal ionizer area is 13.8 cm².

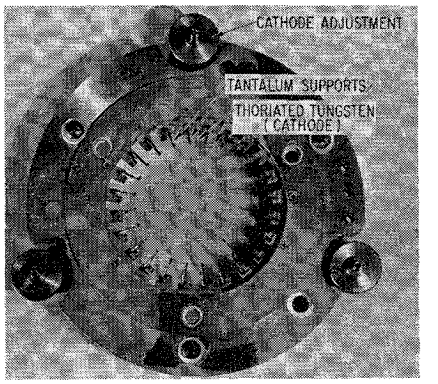

Fig. 5 Cathode assembly, consisting of circular thoriated-tungsten ribbon, spot-welded to tantalum wire supports.

Ionizer and Cathode

Several ionizers were constructed for this experiment. Except for small differences in the arrangement of the cesium vapor feed tube, all ionizers were of nearly identical construction and consisted of an electron-beam welded assembly of a porous tungsten plug with an annular tungsten manifold (Fig. 4). The porous tungsten plug was pressed and sintered from 5.4-μ-diam spherical powder, with a final density of 80% of solid tungsten. The transmission coefficient of the porous tungsten was 5.0×10^{-5}, measured with helium. The nominal porous-tungsten cross-sectional area was 13.8 cm².

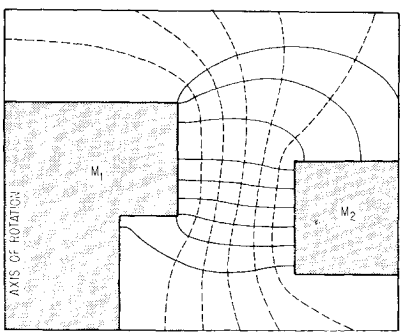

Fig. 6 Computer solution showing magnetic lines of force (solid curves) and equipotential lines (dashed curves) for vacuum field. Case shown is for large axial displacement of pole pieces, resulting in overcompensation of natural slope of field lines in the air gap. (M_1 = inner pole piece, M_2 = outer pole piece.)

Particular care was taken to maintain the ionizer surface as nearly planar as possible. In all cases, the ionizer surface differs by less than ± 0.003 in. from a true plane. A close tolerance is necessary because the accelerating gap is so small.

The cathode filament consists of a circular thoriated tungsten ribbon of 0.002-in. thickness and 0.050-in. width, and is supported by twenty-four tantalum wires that also serve as current leads (Fig. 5). The diameter of the cathode exceeds the outer diameter of the ion-beam.

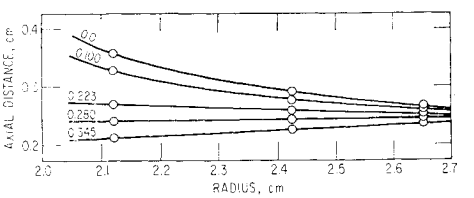

Fig. 7 Magnetic field lines mapped by electron beam method, for various adjustments of the pole pieces.

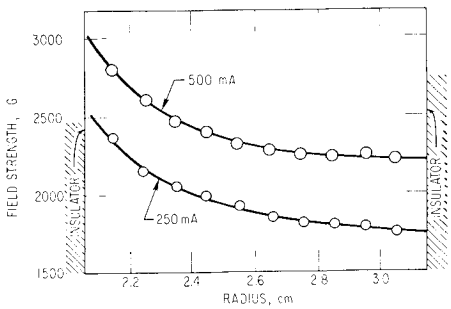

Fig. 8 Magnetic field strength at the ionizer surface, for two values of the solenoid current.

Magnetic Field Configuration

In order to minimize electron drain to the anode, the magnetic field at the ionizer should be exactly parallel to the surface where the contact ionization takes place. In the present apparatus, this is accomplished by properly shaping the pole pieces. If the inner and outer poles were aligned in a single plane normal to the axis of symmetry, the magnetic lines of force would tend to deviate in the direction toward the center of the solenoid, as they approach the axis. This effect can be compensated by letting the inner pole piece protrude (Fig. 6).

The vacuum magnetic field in the vicinity of the air gap (where the ionizer is placed) was determined numerically, by a computer solution of Laplace's equation in cylindrical coordinates. The calculation assumes infinite permeability of the pole pieces. In Fig. 6, the magnetic field lines are traced as solid curves and the equipotential surfaces are dashed curves. By properly adjusting the relative axial displacement of the pole pieces, the magnetic field can be aligned accurately with the ionizer surface. The accuracy is comparable to or better than the tolerance achieved in the construction of the ionizer. Accuracy of the magnetic field alignment was checked by emitting electrons from a small filament located near the edge of the air gap and collecting the electrons with a small probe at several stations along any given magnetic field line.[2] Figure 7 shows a number of field lines in the air gap traced out by this experimental method. The different lines shown correspond to various adjustments of the relative axial position of the pole pieces. The measured field strength on the surface of the ionizer is plotted in Fig. 8.

The performance of the cathode in the presence of the magnetic field, but without the ion-beam, was measured by means of an electrostatic probe. The probe, which was located adjacent to the inner pole piece, traversed the electron sheath produced by the cathode. The final cathode configuration, which was used in all subsequent tests, gave the characteristic shown in Fig. 9.

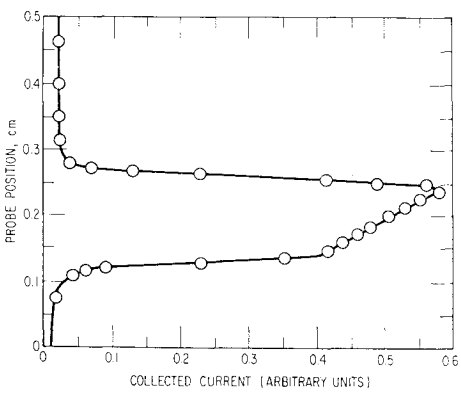

Fig. 9 Probe current vs axial probe position, for final cathode design.

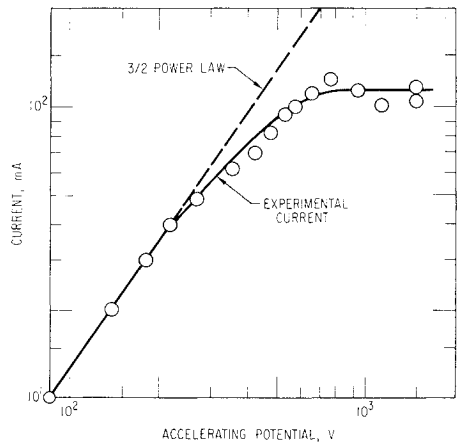

Fig. 10 Ion beam current vs accelerating potential, for constant cesium vapor pressure (21.8 torr), ionizer temperature (1150°C), magnetic induction (2060 gauss at center of ionizer), and gap setting (2.03 mm).

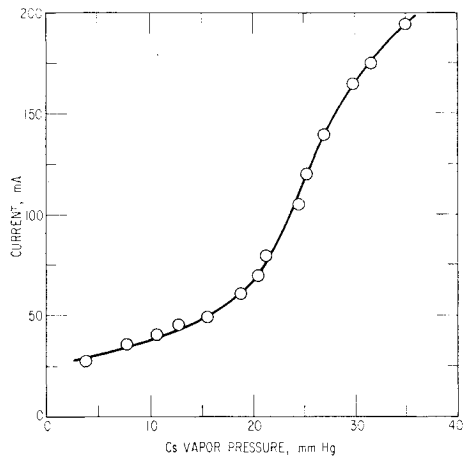

Fig. 11 Ion beam current vs cesium vapor pressure, for constant accelerating potential (1500 v); other conditions same as Fig. 10.

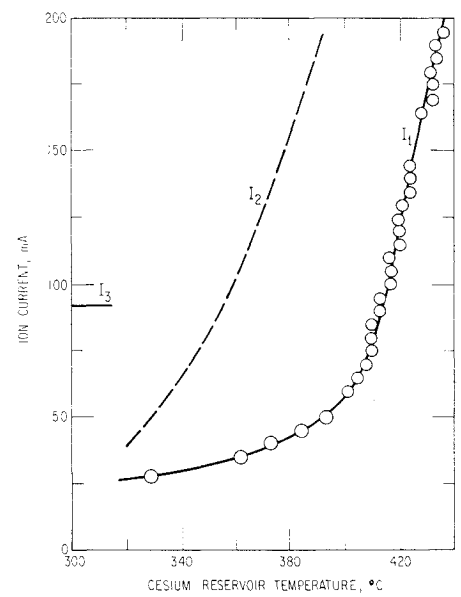

Fig. 12 Ion beam current vs cesium reservoir temperature in representative test series (I_1 = measured current; I_2 = theoretical emission-limited ion current; I_3 = theoretical space-charge-limited ion current).

Table 1 Space-charge-sheath thruster data

	Representative test performance	Maximum value tested
Accelerating gap (ionizer/cathode axial separation), mm	2.03	3.00
Accelerating potential, v	1500	2000
Ionizer outer diam, cm	5.817	5.817
inner diam, cm	3.851	3.851
nominal emitting area, cm^2	13.8	13.8
Temperature of ionizer, °C	1150	1220
Temperature of cathode filament, °C	1835	2050
Magnetic field strength in center of gap, gauss	2060	2500
Reservoir cesium vapor pressure, torr	21.8	38
Ion current, ma	82–113[a]	195
Electron drain current, ma	50–55[a]	>300

[a] Depending on surface condition of ionizer

Performance of the Space-Charge-Sheath Thruster

A large number of tests were conducted, for various values of the accelerating potential, cesium vapor pressure, ionizer and cathode temperatures, magnetic field strength, and anode/cathode axial gap. Measurements made included the determination of the ion beam current and the electron drain

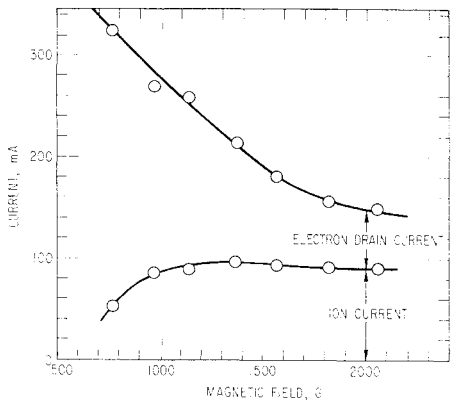

Fig. 13 Ion beam current and electron drain current to anode (ionizer) vs magnetic field at center of ionizer. Accelerating potential = 1500 v, cesium vapor pressure = 21.8 torr, ionizer temperature = 1150°C, gap setting = 2.03 mm.

current to the ionizer. Representative data are given in Table 1.

In these tests, the cesium ion beam was intercepted by a liquid-nitrogen cooled collector. In most tests, biased grids were used to suppress the effect of secondary electrons on the measurement of the ion current.

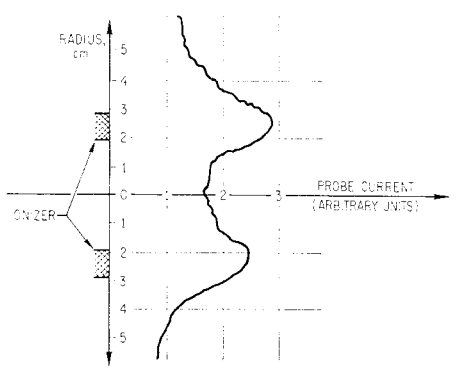

Fig. 14 Experimental probe current vs ion-beam radius, recorded on *x-y* plotter. Probe traverse is along a beam diameter.

As a function of accelerating potential, the ion beam current is at first space-charge limited, but at an increased accelerating potential approaches a constant value determined by the cesium vapor pressure and ionizer temperature (Fig. 10). The dependence of the beam current on cesium vapor pressure is shown in Fig. 11 for the conditions listed.

The measured ion current I_1 is shown in Fig. 12 as a function of the cesium reservoir temperature, for typical operating conditions. The theoretical, emission-limited ion current I_2 shown is calculated on the basis of the cesium vapor pressure and the experimentally determined ionizer transmission coefficient. Also shown for comparison is the theoretical space-charge-limited ion current I_3. At sufficiently large values of the ion current, the measured current exceeds the space-charge limited current, an effect that is due to the partial space-charge compensation provided by the electrons in the accelerating region.

At low magnetic field strength, the electron drain current to the ionizer greatly exceeds the ion current, but becomes progressively smaller at the higher field strengths (Fig. 13). The electron drain current, of course, reduces the efficiency of the device as an electric thruster. (The energy lost appears, however, as heat added to the ionizer, which in most cases must be heated electrically.) The smallest relative electron drain current observed was 31% of the total current (ion plus electron current).

The power loss resulting from the electron drain current varied from 75 to 82 w in the test summarized in Table 1, corresponding to a loss of 730 to 910 ev per beam ion. No attempt was made in these experiments to minimize the heat loss from the ionizer (310 w) or the power consumption of the solenoid (approximately 100 w).

The ion-beam spread was measured by means of a traversing electrostatic probe. The probe principally consists of a small (0.216-in.-diam.) platinum disc. Traversing the ion beam along a diameter, the double-humped profile in Fig. 14 was obtained. The angular spread of the ion-beam is surprisingly small; its half-angle is approximately 1.5°. The same result is also obtained from the erosion pattern

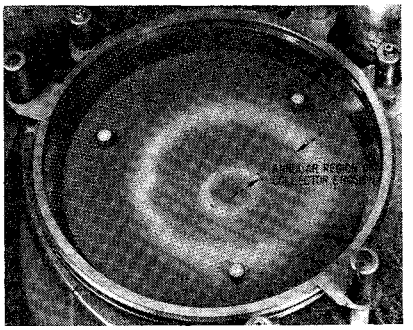

Fig. 15 Annular erosion pattern on beam collector plate.

formed on the ion-beam collector (Fig. 15) at the spot where the ion beam impinges.

An interesting observation, which was made accidentally during testing of the laboratory prototype, was that the thruster could be operated, albeit at reduced performance, with no heater current supplied to the cathode filament. It appears that the tungsten filament becomes partially cesiated, and the lowered work function together with the heating provided by radiation from the ionizer is sufficient to produce the required electron emission.

References

[1] Meyer, R. X., "A Space-Charge-Sheath Electric Thrustor," *AIAA Journal*, Vol. 5, No. 11, Nov. 1967, pp. 2057–2059.

[2] Meyer, R. X., "The Acceleration of Cesium Ions by Means of a Negative Space Charge Sheath," AIAA Paper 66-256, San Diego, Calif., 1966.

[3] Janes, G. S., Dotson, J., and Wilson, T., "Momentum Transfer Through Magnetic Fields," *Proceedings of the Third Symposium on Advanced Propulsion Concepts*, Vol. 1, Gordon and Breach, New York, 1963, pp. 153–176.

[4] Meyerand, R. C., "Momentum Transfer Through the Electric Fields," *Proceedings on the Third Symposium on Advanced Propulsion Concepts*, Vol. 1, Gordon and Breach, New York, 1963, pp. 177–197.

[5] Cann, G. L. and Marlotte, G. L., "Hall Current Plasma Accelerator," *AIAA Journal*, Vol. 2, No. 7, July 1964, pp. 1234–1241.

[6] Pinsley, E. A., "Preliminary Design Considerations of a High-Performance Hall-Current Accelerator," AIAA Paper 65-300, San Francisco, Calif., 1965.

[7] Chubb, D. L. and Seikel, G. R., "Basic Studies of A Low Density Hall Current Ion Accelerator," AIAA Paper 66-76, New York, 1966.

MARCH 1970 J. SPACECRAFT VOL. 7, NO. 3

Effect of Background Pressure on Magnetoplasmadynamic Thruster Operation

R. J. Sovie* and D. J. Connolly†
NASA Lewis Research Center, Cleveland, Ohio

The effect of environmental pressure on magnetoplasmadynamic (MPD) thruster operation was studied. Spectroscopic data indicated no significant effect for pressures below 2×10^{-4} torr. Above this pressure, the effects of collisions between the propellant and background gas were detected; that is, the exit velocity of the primary propellant was reduced. The entrainment and acceleration of background gas was also noticeable above this pressure. Both effects increased in magnitude with increasing tank pressure. It can be seen from the data in at least one case that entrainment seemed to contribute a majority of the thrust at a pressure of 0.2 torr.

Introduction

EFFICIENCIES reported for magnetoplasmadynamic (MPD) thrusters are presently subject to certain reservations.[1] Foremost among these is the expectation that the testing environment, i.e., the presence of background gas, might substantially affect thruster operation. The available data on this subject[2–5] leads to no clear conclusion, and even seems contradictory. In the results of Jones and Walker,[2] the thrust decreased monotonically with increasing tank pressure. In the results of Cann et al.[3,4] there is a minimum in the thrust against tank pressure curves with a net increase in thrust as one goes from very low to very high pressure. The results of Bennett et al.[5] were generally consistent with those of Jones and Walker. In all of these studies the measurements reported were limited to tank pressure, thrust, and thruster operating parameters.

The present study attempts to determine if both types of results described previously are reproducible, and, if so, in what regimes each applies. This study also incorporates beam diagnostics to examine the nature of the thruster-environment interaction. The axial velocities of both the primary propellant and the background gas were measured by a spectroscopic Doppler shift technique.[6]

Presented as Paper 69-243 at the AIAA 7th Electric Propulsion Conference, Williamsburg, Va., March 3–5, 1969; submitted March 4, 1969; revision received September 3, 1969.

* Physicist.

† Aerospace Research Engineer.

Apparatus and Measurement Techniques

All experiments were performed in a 15-ft-diam, 65-ft-long vacuum tank.[7] The work was done with the water-cooled thruster[2,8,9] shown in Fig. 1. The thrust measurements were made using a parallelogram-pendulum thrust stand. The electrical power to the thruster was brought onto the stand through coaxial lines terminated on coaxial mercury pots. The power was supplied by commercial welding power supplies. Deflection of the stand was sensed by a linear differential transformer with output indicated on a strip chart recorder. The system was calibrated by a weight and pulley

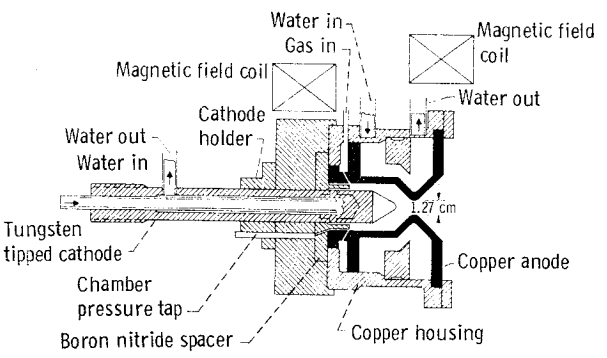

Fig. 1 Schematic of water cooled MPD arc thruster.